

## Neutron inelastic cross section measurements on $^{54}\text{Fe}$

Adina Olacel<sup>1,\*</sup>, Catalin Borcea<sup>1</sup>, Marian Boromiza<sup>1</sup>, Philippe Dessagne<sup>2</sup>, Gregoire Henning<sup>2</sup>, Maëlle Kerveno<sup>2</sup>, Luiz Leal<sup>3</sup>, Alexandru Negret<sup>1</sup>, Markus Nyman<sup>4</sup>, and Arjan Plompen<sup>4</sup>

<sup>1</sup>Horia Hulubei National Institute for Physics and Nuclear Engineering, Reactorului 30, 077125 Bucharest-Măgurele

<sup>2</sup>Université de Strasbourg, CNRS, IPHC UMR 7178, Strasbourg, France

<sup>3</sup>Institut de Radioprotection et de Sécurité Nucléaire, BP 17 – 92262 Fontenay-aux-Roses Cedex, France

<sup>4</sup>European Commission, Joint Research Centre, Retieseweg 111, B – 2440 Geel, Belgium

**Abstract.** A  $^{54}\text{Fe}(n, n'\gamma)$  cross section measurement was performed at the Geel Electron LINear Accelerator of EC-JRC, Geel using the Gamma Array for Inelastic Neutron Scattering spectrometer and a  $^{235}\text{U}$  fission chamber for flux normalization. The experimental results are presented in comparison with TALYS 1.9 default and tuned calculations. The tuned calculation, implying modifications of the optical model parameters, improved significantly the description of the experimental values and led to interesting conclusions regarding the interaction of the  $^{54}\text{Fe}$  nucleus with neutrons. Since the results of these calculations were already presented extensively in a dedicated paper, the present article focuses on details related to the experimental particularities and data analysis procedure.

### 1 Introduction

Iron is an important structural material in the design of the nuclear facilities. Being a component material of stainless steel, reporting precise and reliable neutron inelastic data impacts on the criticality and safety assessments. The importance of iron is highlighted in the High Priority Request List (HPRL) [1] and also in the Collaborative International Evaluated Library Organization (CIELO) project [2–4] of the Nuclear Energy Agency (NEA). Both of them emphasize primary on the need of neutron inelastic data on  $^{56}\text{Fe}$  but acknowledge also the importance of the data on  $^{54}\text{Fe}$  and  $^{57}\text{Fe}$ , even if they represent only 5.85(11)% and 2.12(3)%, respectively, of the natural iron [5]. A few years ago our group started a measurement campaign which focuses on these 3 stable isotopes of iron.

The first measurement was on  $^{56}\text{Fe}$ . The results were published in Ref. [6] in comparison with previously reported data and theoretical calculations performed using the TALYS code [7]. It was concluded that the agreement is better when using the default input parameters than the ones deduced from a more microscopic approach.

The next measurement was on  $^{57}\text{Fe}$ . This proved to be challenging because the main transition, decaying from a very low-lying level ( $E_L = 14.41$  keV), could not be detected [8]. Therefore, dedicated theoretical calculations were performed in order to complement the available experimental information. We also found significant discrepancies with previous data [8]. Therefore, a new experiment was performed using the GRAPhEME (GeRmanium array for Actinides PrEcise MEasurements) spectrometer [9–11]. This is a setup especially designed for

inelastic neutron scattering measurements on actinides and was suitable for detecting also the 14-keV  $\gamma$  ray. The data analysis of this experiment is currently ongoing.

The latest measured iron isotope was  $^{54}\text{Fe}$ . The experimental results obtained following the inelastic scattering of neutrons on  $^{54}\text{Fe}$  were published in Ref. [12] in comparison with previously reported results and with two TALYS theoretical calculations. The first calculation was done using the default input parameters. As the agreement between the experimental results and the default theoretical predictions was bad we performed a tuned calculation by modifying the optical model parameters. The modifications were done for the radius associated with the proton volume-central term and the diffuseness and the radius of the neutron surface-central component. The challenge was to do this by keeping the total, the elastic and the most relevant reaction cross sections ( $(n, p)$  and  $(n, \alpha)$ ) within experimental limits. Ref. [12] presents detailed information on how the modifications were done and how they affected the values of the inelastic cross sections. This paper focuses on particularities related to the experiment and the data analysis procedure.

### 2 Experimental setup

The experiment was performed at the Geel Electron LINear Accelerator (GELINA) white neutron source [13] using the Gamma Array for Inelastic Neutron Scattering (GAINS) spectrometer [14] for detecting the  $\gamma$  rays and a  $^{235}\text{U}$  fission chamber (FC) [15] for flux monitoring. GAINS consists of 12 HPGe detectors placed at  $110^\circ$ ,  $125^\circ$  and  $150^\circ$  with respect to the beam direction, with four detectors at each angle (see Fig. 1). The FC is placed

\*e-mail: aolacel@tandem.nipne.ro

Table 1: Characteristics of the  $^{54}\text{Fe}$  sample used in the experiment.

Isotopic concentration	$^{54}\text{Fe}$ - 97.68(7)% $^{56}\text{Fe}$ - 2.24(6)% $^{57}\text{Fe}$ - 0.04(1)% $^{58}\text{Fe}$ - 0.04(1)%
mass	19.494(10) g
diameter	51.00(51) mm
thickness	1.30(1) mm
areal density	0.933(18) g/cm <sup>2</sup>

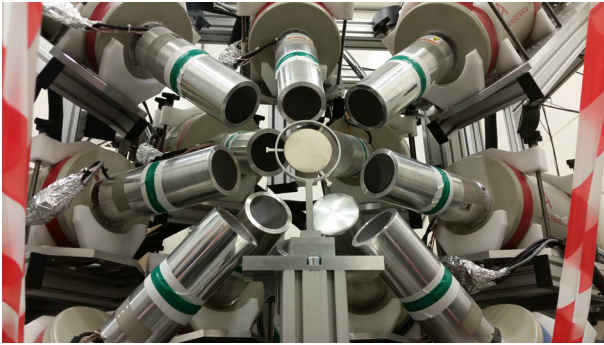


Figure 1: The GAINS spectrometer.

211.5 cm upstream the sample and contains 8 uranium layers of 70 mm diameter on five Al foils of 20- $\mu\text{m}$  thickness supported by a 84-mm diameter ring. The enriched  $^{54}\text{Fe}$  sample, with characteristics presented in Table. 1, was leased from the Isotope Office of the Oak Ridge National Laboratory. The diameter of the sample (51 mm) was smaller than the diameter of the beam (61 mm) and of the fission chamber deposits (70 mm). Because of that, in order to take into account any potential irregularities in the shape of the  $^{54}\text{Fe}$  sample we increased the areal density uncertainty to 2%. The experiment was performed at 100 m distance from the neutron source which resulted in a neutron energy resolution of 3 keV at 1 MeV and 80 keV at 10 MeV. The data acquisition was digital for the HPGe detectors and analog for the fission chamber.

### 3 Data analysis procedure

In order to determine the primary data, which are the  $\gamma$ -production cross sections, we analyse the data from both the HPGe detectors and the fission chamber. The data analysis of the HPGe detectors is extensively described in Refs. [16–18]. Some important features of the fission chamber data analysis will be further discussed here. Figure 2 displays the fission chamber amplitude spectrum. The low-energy peak is caused by  $\alpha$  particles emitted during the decay of  $^{235}\text{U}$  and is separated by a plateau from the region corresponding to the neutron-induced fission events. In order to determine the efficiency of the fission chamber we apply in the middle of the plateau a software threshold to reject the  $\alpha$  events. However, some fission fragments will produce low amplitude pulses. Therefore,

the total number of fission events is calculated by extrapolating the plateau to zero pulse height. Figure 2 shows the extrapolation and indicates the quantities ( $I_1$ ,  $I_2$ ) used to calculate the efficiency of the fission chamber. This is calculated using the formula:

$$\epsilon_{FC} = \frac{I_1}{I_1 + I_2} \quad (1)$$

assuming an uncertainty of 50% for  $I_2$ .

Further corrections are applied for:

- the polarity effect of the fission chamber ( $C_1$ ) [15];
- the number of the fission chamber fragments that stop in the deposit ( $C_2$ ) [19],
- the inhomogeneity of the  $\text{U}_F4$  foils ( $C_3$ ) [20].

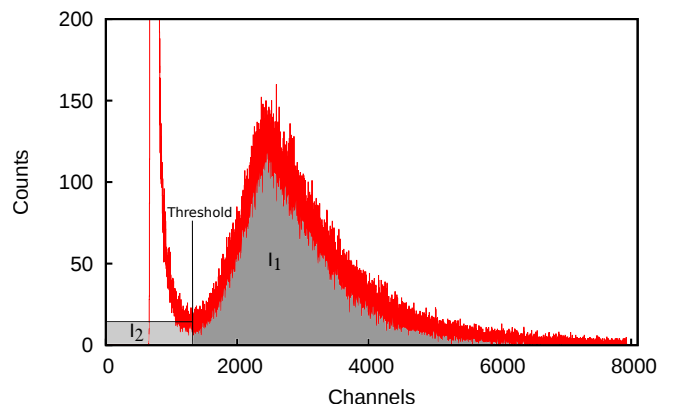


Figure 2: The amplitude spectrum recorded with the fission chamber in the  $^{54}\text{Fe}$  experiment. The sum of  $I_1$  and  $I_2$  represents the total number of the neutron-induced fission events.

After all these corrections the final efficiency of the fission chamber is calculated as:

$$\epsilon_{FC} = \frac{I_1}{I_1 + I_2} \times C_1 \times C_2 \times C_3 \quad (2)$$

The procedure used to determine the efficiency of the fission chamber was validated by an experiment carried out at the Physikalisch-Technische Bundesanstalt Institute (PTB) [21], during which the neutron sensitivity of the fission chamber was found to be in a very good agreement with the proton recoil telescope of PTB. The efficiency of the fission chamber in the current experiment was calculated to be 85(2)%.

The primary data, which are the differential  $\gamma$ -production cross sections are determined using the following formula:

$$\frac{d\sigma_j}{d\Omega}(\theta_i, E_k) = \frac{1}{4\pi} \frac{Y_j(E_k)}{Y_{FCj}(E_k)} \frac{\epsilon_{FC} \sigma_U(E_k) t_U A_s}{\epsilon_j t_s A_U c_{ms}(E_k)} \quad (3)$$

where  $\theta$  is the angle of the detector,  $E_k$  is the incident neutron energy for the bin  $k$ ,  $Y_j$  is the  $\gamma$ -ray yield from HPGe detector  $j$ ,  $Y_{FCj}$  is the FC yield corresponding to detector  $j$ ,  $\epsilon_j$  is the  $\gamma$  efficiency of detector  $j$ ,  $\sigma_U$ , the  $^{235}\text{U}(n,f)$  cross

section,  $t_U$  the thickness of the  $^{235}\text{U}$  deposit,  $t_s$  the sample thickness,  $A_U=235.04$  and  $A_s=53.93$  are the atomic masses of  $^{235}\text{U}$  and  $^{54}\text{Fe}$ , respectively and  $c_{ms}$  the multiple scattering correction factor.

The  $\gamma$ -production cross section for each transition is calculated by integrating the cross section based on the differential cross section values at  $110^\circ$  and  $150^\circ$  using the following expression:

$$\sigma(E_k) = 2\pi[w_{110^\circ} \frac{d\sigma}{d\Omega}(110^\circ, E_k) + w_{150^\circ} \frac{d\sigma}{d\Omega}(150^\circ, E_k)] \quad (4)$$

where  $\frac{d\sigma}{d\Omega}(110^\circ, E_k)$  and  $\frac{d\sigma}{d\Omega}(150^\circ, E_k)$  are the differential  $\gamma$ -production cross sections. The angle integration coefficients are  $w_{110^\circ}=1.30429$  and  $w_{150^\circ}=0.69571$ .

## 4 Results

Figure 3 displays the  $\gamma$ -production cross section of the main transition in  $^{54}\text{Fe}$  with  $E_\gamma = 1408.1$  keV. The experimental values (black line) are displayed together with the uncertainties (gray band) and are compared with two TALYS theoretical calculations. The need of the second (tuned) calculations was underlined by the bad agreement between the experimental results and the default calculations. Extensive description of the calculations is available in Ref. [12]. The experimental cross section has a relatively well defined shape with a maximum value around 950 mb and a plateau extended over a large incident energy range where cross section stays constant to  $\approx 700$  mb up to 12 MeV. The values are reported with an uncertainty under 5% for most of the incident energy range. This, together with the other  $\gamma$ -production cross sections are discussed in Ref. [12].

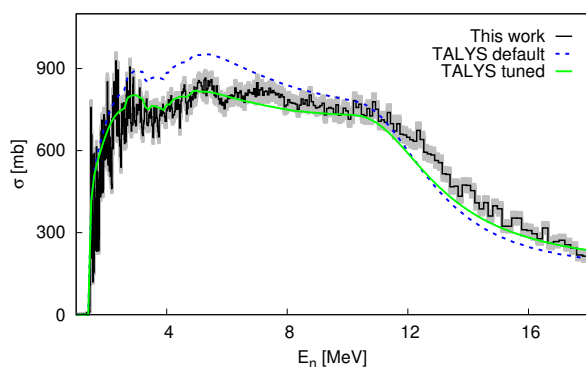


Figure 3: The  $\gamma$ -production cross section of the main transition in  $^{54}\text{Fe}$  with  $E_\gamma=1408.1$  keV. The gray band represents the total uncertainty.

## 5 Conclusions

We presented some specific details of the analysis procedure of a  $^{54}\text{Fe}(n, n'\gamma)$  cross section measurement performed at GELINA using the GAINS spectrometer. In particular, we describe the data analysis concerning the

determination of the fission chamber efficiency, which is necessary for monitoring the incident neutron flux. This is a very general procedure used in the data analysis of all the neutron inelastic scattering experiments performed using the GAINS spectrometer and the GELINA neutron source. We also display the results for the  $\gamma$ -production cross section of the main transition in  $^{54}\text{Fe}$  in comparison with two TALYS theoretical calculations [12].

This work was supported by the European Commission within the Seventh Framework Program through Fission-2013-CHANDA (project no. 605203) and by the Ministry of Research and Innovation of Romania, CNCS-UEFISCDI, through project no. PN-III-P4-ID-PCE-2016-0025 within PNCDI III. The authors acknowledge the support team of the GELINA facility for providing the conditions of the experiment.

## References

- [1] High Priority Request List, <https://www.oecd-neia.org/dbdata/hprl>, [Online accessed 02-July-2019]
- [2] Nuclear Energy Agency, OECD, Collaborative International Evaluated Library Organisation (CIELO) Pilot Project, WPEC Subgroup 40 (SG40), <https://www.oecd-neia.org/science/wpec/sg40-cielo>, [Online accessed 02-July-2019].
- [3] M.B. Chadwick, R. Capote, A. Trkov, M.W. Herman, D.A. Brown, G.M. Hale, A.C. Kahler, P. Talou, A.J. Plompen, P. Schillebeeckx, M.T. Pigni, L. Leal, Y. Danon, A.D. Carlson, P. Romain, B. Morillon, E. Bauge, F.-J. Hamsch, S. Kopecky, G. Giorginis, T. Kawano, J. Lestone, D. Neudecker, M. Rising, M. Paris, G.P.A. Nobre, R. Arcilla, O. Cabellos, I. Hill, E. Dupont, A.J. Koning, D. Cano-Ott, E. Mendoza, J. Balibrea, C. Paradela, I. Durán, J. Qian, Z. Ge, T. Liu, L. Hanlin, X. Ruan, W. Haicheng, M. Sin, G. Noguere, D. Bernard, R. Jacqmin, O. Bouland, C. De Saint Jean, V.G. Pronyaev, A.V. Ignatyuk, K. Yokoyama, M. Ishikawa, T. Fukahori, N. Iwamoto, O. Iwamoto, S. Kunieda, C.R. Lubitz, M. Salvatores, G. Palmiotti, I. Kodeli, B. Kiedrowski, D. Roubtsov, I. Thompson, S. Quaglioni, H.I. Kim, Y.O. Lee, U. Fischer, S. Simakov, M. Dunn, K. Guber, J.I. Márquez Damián, F. Cantargi, I. Sirakov, N. Otuka, A. Daskalakis, B.J. McDermott, and S.C. van der Marck, Nucl. Data Sheets 148, 189 (2018).
- [4] M. Herman, A. Trkov, R. Capote, G.P.A. Nobre, D.A. Brown, R. Arcilla, Y. Danon, A. Plompen, S.F. Mughabghab, Q. Jing, G. Zhigang, L. Tingjin, L. Hanlin, R. Xichao, L. Leal, B.V. Carlson, T. Kawano, M. Sin, S.P. Simakov, and K. Guber, Nucl. Data Sheets 148, 214 (2018).
- [5] J. Meija, T. B. Coplen, M. Berglung, W. A. Brand, P. De Bièvre, M. Gróning, N. E. Holden, J. Irrgeher, R. D. Loss, T. Walczyk, and T. Prohaska, Pure Appl. Chem. 88(3), 293-306 (2016).
- [6] A. Negret, C. Borcea, Ph. Dessagne, M. Kerveno, A. Olacel, A. J. M. Plompen, and M. Stanoiu, Phys. Rev. C 90, 034602 (2014).

- [7] A.J. Koning, S. Hilaire, M.C. Duijvestijn, TALYS-1.0, in Proceedings of the International Conference on Nuclear Data for Science and Technology, April 22-27, 2007, Nice, France, edited by O. Bersillon, F. Gunsing, E. Bauge, R. Jacqmin, S. Leray (EDP Sciences, 2008) pp. 211–214.
- [8] A. Negret, M. Sin, C. Borcea, R. Capote, Ph. Dessagne, M. Kerveno, N. Nankov, A. Olacel, A. J. M. Plompen, and C. Rouki, Phys. Rev. C 96, 024620 (2017).
- [9] M. Kerveno, A. Bacquias, C. Borcea, Ph. Dessagne, G. Henning, L.C. Mihailescu, A. Negret, M. Nyman, A. Olacel, A.J.M. Plompen, C. Rouki, G. Rudolf, J.C. Thiry, Eur. Phys. J. A 51, 167, (2015).
- [10] M. Kerveno, J.C. Thiry, A. Bacquias, C. Borcea, P. Dessagne, J.C. Drohé, S. Goriely, S. Hilaire, E. Jericha, H. Karam, A. Negret, A. Pavlik, A.J.M. Plompen, P. Romain, C. Rouki, G. Rudolf, M. Stanoiu, Phys. Rev. C 87, 24609 (2013).
- [11] Maëlle Kerveno, Marc Dupuis, Catalin Borcea, Marian Boromiza, Roberto Capote, Philippe Dessagne, Greg Henning, Stéphane Hilaire, Toshihiko Kawano, Alexandru Negret, Markus Nyman, Adina Olacel, Eliot Party, Arjan Plompen, Pascal Romain and Mihaela Sin in Proceedings of International Conference on Nuclear Data for Science and Technology, Beijing, China, 2019.
- [12] A. Olacel, C. Borcea, M. Boromiza, Ph. Dessagne, G. Henning, M. Kerveno, L. Leal, A. Negret, M. Nyman, and A.J.M. Plompen, Eur. Phys. J. A 54:183 (2018).
- [13] D. Ene, C. Borcea, S. Kopecky, W. Mondelaers, A. Negret, A.J.M. Plompen, Nucl. Instrum. Methods Phys. Res. A 618, 54 (2010).
- [14] D. Deleanu, C. Borcea, Ph. Dessagne, M. Kerveno, A. Negret, A.J.M. Plompen, J.C. Thiry, Nucl. Instrum. Methods Phys. Res. 624, 130 (2010).
- [15] A. Plompen, N. Nankov, C. Rouki, M. Stanoiu, C. Borcea, D. Deleanu, A. Negret, Ph. Dessagne, M. Kerveno, G. Rudolf, J.C. Thiry, M. Mosconi, R. Nolte, J. Korean Phys. Soc. 59, 1581 (2011).
- [16] L.C. Mihailescu, L. Oláh, C. Borcea, A.J.M. Plompen, Nucl. Instrum. Methods Phys. Res. A 531, 375 (2004)
- [17] C. Rouki, P. Archier, C. Borcea, C. de Saint Jean, J.C. Drohé, S. Kopecky, A. Moens, N. Nankov, A. Negret, G. Noguère, A.J.M. Plompen, M. Stanoiu, Nucl. Instrum. Methods Phys. Res. A 672, 82 (2012).
- [18] A. Olacel, C. Borcea, P. Dessagne, M. Kerveno, A. Negret, A.J.M. Plompen, Phys. Rev. C 90, 034603 (2014).
- [19] C. Butz-Jorgensen, H.-H. Knitter, and G. Bortels, Nucl. Instrum. Methods Phys. Res. 236, 630 (1985).
- [20] P. Schillebeeckx, A. Borella, J. C. Drohe, R. Eykens, S. Kopecky, C. Massimi, L. C. Mihailescu, A. Moens, M. Moxon, and R. Wynants, Nucl. Instrum. Methods Phys. Res. A613, 378 (2010).
- [21] M. Mosconi, R. Nolte, A. Plompen, C. Rouki, M. Kerveno, P. Dessagne, J.C. Thiry, Characterisation of fission ionisation chambers using monoenergetic neutrons, EFNUDAT Workshop, Geneva, Switzerland, 2010.